A Statistical Wavelet-Based Process for Systems Catastrophic Failure Precursor Detection

Ousmane Diallo[1], Dimitri Mavris, PhD[1]

[1] *Georgia Institute of Technology, Atlanta, Georgia, 3033, USA*
ousmane.diallo@gatech.edu
dimitri.mavris@ae.gatech.edu

ABSTRACT

As a consequence of the recent deregulation in the electrical power production industry, new private entrepreneurs with no prior experience in the power plant operation have entered into the power generation business. They hedge the business risks by outsourcing the operation and maintenance activities to third party service providers with whom they share risks/rewards of plant performance. The main maintenance providers are the original equipment manufacturers, who are responsible for the majority of the cost associated with unplanned outages. With the cost-benefit of preventing such unplanned outage as a gas turbine compressor failure hovering around the twenty million dollars mark, techniques for detecting failure precursors to avoid or limit the number of systems catastrophic failure are necessary. In this paper, a methodical process is proposed to detect precursory events that lead to catastrophic systems failure. The wavelet packet transform is used to perform multi-resolution analysis of gas turbines health, condition and vibration sensors data to extract their signal features. Then the probabilistic principal component analysis is utilized to fuse them into a few uncorrelated variables. Next a one-dimensional signal representing the multi-variables data is computed. After that the statistical process control techniques is applied to set the anomaly threshold. Finally, a Bayesian hypothesis testing method is applied for abnormality detection to the monitored signal. As a proof of concept, the proposed process is successfully applied to a gas turbine compressor failure precursor detection.*

1 INTRODUCTION

As a consequence of the recent deregulation in the electrical power production industry, there has been a shift in the traditional ownership of power plants and the way they are operated. Many new private entrepreneurs with no prior experience in power plant operation have invested into the power plant business. Thus, to hedge their business risks, those private entrepreneurs enter into long-term service agreement (LTSA) with third parties for their operation and maintenance (O&M) activities. Thereby, the original equipment manufacturers (OEMs) become the natural choices as third party O&M providers because they know and understand their designed products best and will be willing to guarantee their operations. Each of these main gas turbine OEMs (together they represent about 94% of the global market (Thaler 2006)) has its own set of definitions and foreseeable benefits to the plant owners of their LTSA offerings. Thus, the major OEMs have invested huge amounts of money to develop preventive maintenance strategies to minimize the occurrence of the normally costly unplanned outages resulting from failures of equipment covered under LTSA contracts.

The high potential for cost benefits to gas turbine OEMs when failures can be prevented raises the importance of techniques for detecting faults in gas turbines. In this paper, a systematic process is proposed that can successfully detect failure precursory events. The remaining of the paper is organized as follow: Section 2 sets the context and background regarding power plant O&M and the background for the problem addressed. Section 3 presents the steps of the proposed approach to detect catastrophic failure precursors. Then an illustrative example of application to a gas turbine compressor failure problem is presented in Section 4, followed by a brief conclusion in Section 5.

2 POWER PLANT O&M BACKGROUND

Typically, the LTSA contracts work like insurance policies where the manufacturer guarantees a given level of power output and/or efficiency over several years. Also they may provide repair, replacement, and upgrade parts to the degrading power plant. Overall, it is supposed to be a “win-win” partnership for both parties, wherein they share the operational risks as well as the rewards of extra performance generated by the power plant. Another advantage of entering into LTSA, it is well accepted in the power generation field that LTSA contracts raise the plant re-sale value while, for the OEM, the equipment under contract provides unprecedented access to “a live laboratory” that should allow the OEM to learn from eventual design shortcomings of previous gas turbine designs in order to improve upon future designs, ultimately giving them a competitive advantage.

2.1 Power plant operation and maintenance

The O&M expenditures of a typical power plant are an important part of the total life cycle cost consisting of 15% to 20%, while equipment maintenance costs account for approximately 10% to 15% (Stoll 2001). To be clear, there is always a cost associated with an outage whether it is planned or unplanned. However, costs involved with planned outages are typically predetermined and planned for within the O&M budget whereas those related to the unplanned ones are not, therefore represent losses. Thus, to make the LTSA contracts profitable, the providers need to reduce the number of unplanned outages because the consequence of such unplanned outages can be expensive. Typically under a LTSA contract, the provider has to pay the plant owners a liquidated damage for each forced outage. In general, the liquidated damage cost for a forced outage includes: the loss of production cost, the repair cost, the cost of buying the equivalent power to meet the quantity that the forced outage plant was dispatched for at usually higher prices, and eventual regulatory penalties**.**

2.2 Problem Background

With the steep cost of potential liquidated damage associated with not meeting the reliability and performance requirement, LTSA providers need to develop strategies so that the revenues from the contracts exceed the cost of the involved risks. In fact, according to a report of the Electric Power Research Institute (EPRI), the cost benefit from preventing a General Electric gas turbine 7FA and 9FA technology compressor failure is estimated to be ten to twenty million dollars (EPRI 2008).

Thus, OEMs have been investing huge amounts of money to develop strategies to avoid unplanned plant outages. For example, OEMs like GE Energy created a Power Answer Center in Atlanta, GA, where all power plants under its LTSA contract are continuously monitored using installed sensors on gas turbine. The illustrative Figure 1 shows the GE Power Answer architecture wherein the on-site monitor compares the actual unit performance with baseline predictions and provides the first level of anomaly detection and notification.

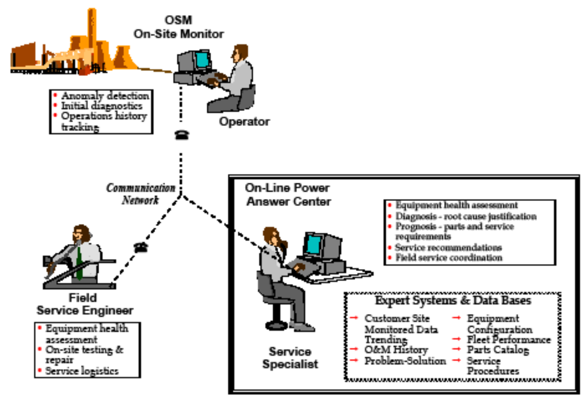

Figure 1: GE Monitoring & Diagnostics concept (Thaler 2006).

Major OEMs like GE have the ability to monitor hundreds of units throughout the world in real time in order to establish knowledge to detect faults before they can develop into failure. This is both challenging and can yield some advantages toward sustaining the technological competitive advantage of an OEM in the long run. Despite all of the effort to avoid forced outages, there are still undetected failure precursors that led to catastrophic failure as reported by EPRI in its 2007 updated report (EPRI 2007).

3 DETECTION OF FAILURE PRECURSORS

Though in recent years, there have been new and improved techniques such as condition-based monitoring (CBM) to help detect anomalies in their early stages of development, currently, the new techniques have not allowed to totally resolve the issue of missed detections of all the anomalies. Although their merit is well accepted, their practical implementation is still inefficient because these techniques tend to be theoretical, difficult, and/or expensive to apply to real world problems. Therefore, the method proposed herein intends to take advantage of the monitoring sensors to capture catastrophic failure precursors.

In general, the health and condition of power plants are monitored using two types of sensors: the static or process-related sensors (used to measure temperature, pressure, and flow), and the sensors characterized by their high-bandwidth used for high-frequency signals like the vibration measurements. Although, there are many time-frequency techniques reported in the literature such as the Wigner-Ville distribution, the Choi-Williams distribution, the short time Fourier transforms; the wavelet transform is the best one to deal with short lasting anomalies and sharp discontinuities (Graps 1995). The following subsections provide a brief overview of the wavelet transform followed by a presentation of a step-by-step explanation of the proposed approach.

3.1 Wavelet transforms overview

The time-frequency analysis techniques are appropriate when dealing with identifying anomalies in time series signals because more information can be extracted about small variations of a signal in the combination of the time and the frequency domains than can be extracted in the time domain alone. The Fourier transform is the most popular frequency domain analysis technique because of its ability to decompose an energy limited signal f(t) so as to analyze the signal in the time domain for its frequency contents F(ω) as defined by Eqs 1 and 2:

$$f(t) = \frac{1}{2\pi}\int_{-\infty}^{\infty} F(\varpi)e^{i\omega t}d\omega \qquad (1)$$

$$F(\omega) = \int_{-\infty}^{\infty} f(t)e^{i\omega t}dt \qquad (2)$$

However, the Fourier transform provides only the global information on the frequencies of a signal, it cannot provide local information if the spectral composition of a signal changes rapidly with time (Misrikhanov 2006). In other words, once a signal is Fourier transformed, all the time domain information is lost, while the wavelet transform conserves both the time and the frequency information. Thus, the wavelet transform is an improvement over Fourier transforms for time-frequency analysis in that context. Wavelet transforms decompose a given signal through two filters: a low-pass filter that provides a low frequency part which trends and smoothes the original signal (i.e., approximation), and a high-pass filter that provides the high frequency part (i.e., details) which reveals local properties such as anomalies.

3.1.1 Mathematical overview of Wavelet Transforms

There are plenty of literature on the theory of wavelet transforms and its applications (Chui 1992; Daubechies 1992). Just like the Fourier transforms, the wavelet transform can be defined for any square-integrable function $L^2(\Re)$ (Wu and Du 1996). But instead of using the harmonics, $e^{i\omega t}$, the wavelet basis, ψ, called a mother wavelet function, is used and defined as:

$$\psi_{a,b}(t) = \frac{1}{\sqrt{a}}\psi\left(\frac{t-b}{a}\right) \qquad (3)$$

Where a is the dilation or scaling parameter and b is the time location or translation parameter. Thus the wavelet transform of a signal f(t) is computed as follows (Chui 1992):

$$W_f(a,b) = \int_{-\infty}^{\infty} f(t)\psi_{a,b}(t)dt \qquad (4)$$

3.1.2 Wavelet Packets

The standard wavelet transforms has limitations because it can only decompose the low-frequency part of a signal. To remedy that limitation, the wavelet packet transform was introduced. It has the ability to decompose both the approximation part as well as the detail part. The wavelet packet transform decomposes a signal into more detailed components than the standard wavelet transform could, thereby yielding more information about the signal. For that reason, it is more advantageous to use the wavelet packet transform to realize the multi-resolution analysis (MRA) by decomposing both the low frequency and high frequency components of a signal into subspaces so as to obtain finer and adjustable resolution (Jiang and Adeli 2004). Figure 2 illustrates a wavelet packet decomposition of a signal S.

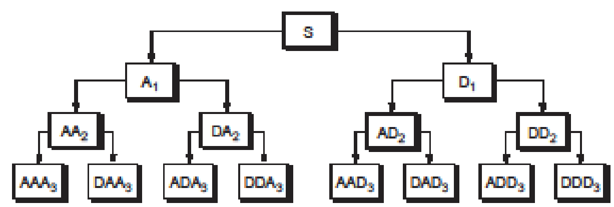

Figure 2: Wavelet packet decomposition (Matlab 1999-2009)

3.2 Steps for failure precursor detection

As mentioned above, the proposed approach intends to take advantage of monitoring sensors to capture catastrophic failure precursors. Figure 3 shows a flowchart of the proposed methodology for intelligent failure precursor detection using multi-resolution analysis. A step-by-step explanation of each block in the flowchart is presented in the subsections below. The different steps of the proposed approach have been explained in (Diallo and Mavris 2010)

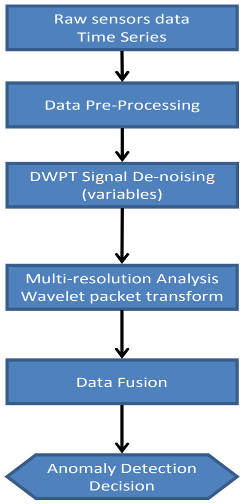

Figure 3: Intelligent failure precursor detection

3.2.1 Raw time series data collection

The systems health and operating condition parameters are continuously monitored and collected using installed sensors and stored for potential post-processing. The installed sensors for heavy-duty gas turbines typically include the two types mentioned previously, static or process-related sensors (used for pressure, temperature, and flow rate measurements) and high-bandwidth sensors used to measure high-frequency measurements (e.g., vibration measurement).

3.2.2 Data Pre-Processing

The pre-processing of the raw data is a necessary step for a couple of important reasons. First, the OEMs will not want to share their proprietary data on equipment malfunctioning because that may affect their competitive advantages due to risk of possibility of reverse engineering. Secondly, the sensors monitor different health parameters (e.g., temperature, pressure, vibration, etc) that are recorded in different units and more importantly in different orders of magnitude. For instance, a typical normal base load operation of GE's 7FA+e gas turbine technology can have a compressor discharge temperature measurement in the range of 600 to 800 degrees Fahrenheit, while the vibration sensor measurements could be on the order of 1/10 of an inch per second. Therefore, an analysis with the raw measurement could be artificially skewed towards the variables with higher absolute values. Thus, the pre-processing step consists of normalizing each measured parameter value by the mean value of that variable measurement, and eliminating the visual outliers that would misrepresent the finding and affect the accuracy of the conclusion.

3.2.3 DWPT signal de-noising

The de-noising step is essential because a sensor measurement signal is always tainted by noise. In (Jiang, Mahadevan et al. 2006) the authors presented a de-noising technique that adequately removes the noise by combining the discrete wavelet packet transform (DWPT) and Bayesian thresholding. The result is the removal of just the noise without the drawbacks of many other de-noising algorithms that either remove useful information along with the noise or remove too little noise thus leaving some noise in the signal.

3.2.4 Multi-resolution analysis using discrete wavelet packet decomposition

In this step, the de-noised signal is decomposed at an appropriate level (3-level) of resolution (as in Figure 2) to get the approximation and the detail components. The content of each component resulting from the decomposition can be analyzed. Once the decomposed tree is obtained, the energy content of the scaling function (approximation) and the wavelet functions (details) representing the nodes of the tree is calculated as:

$$E_{j,n} = \int_{-\infty}^{\infty} \left(W_{j,n,k}(dt)\right)^2 dt = \sum_k W_{j,n,k}^2 \qquad (5)$$

Where: $W_{j,n,k}$ is the wavelet packet transform coefficient, j is the level, k is the translation, and n is the modulation parameter (approximation or detail). The energy content of each node will then be used as the signal features.

3.2.5 Data Fusion using PPCA

The goal of the data fusion step is to combine pieces of information from a system that has potentially correlated multi-sensory data set into fewer uncorrelated variables that allow for drawing a more adequate conclusion than one could get from each individual sensor. Thus, the probabilistic principal component analysis (PPCA) is used to merge the information from the sensors of interest. To perform the PPCA, the steps of the principal components analysis are executed, then the notion of maximum likelihood and the variance of the reduced data is calculated using matrices, where only the most significant weights obtained from the standard PCA are used as entries in a maximum likelihood matrix. The PPCA is an improved version of the standard PCA as it has the advantage of taking into account data uncertainty (Tipping and Bishop 1999).

3.2.6 Anomaly detection decision

The procedure for anomaly detection decision is done in a multi-steps approach.
After completion of the PPCA step, the different principal components of the signal as obtained from PPCA are converted into a one-dimensional signal calculated as follows:

$$RS = \sum_{i=1}^{n} \lambda_k \Phi_k^*(i) \tag{6}$$

n: le number of retained principal components (PC)
λ_k : The contribution of the k^th Eigenvalues
$\Phi_k^*(i)$: The signal corresponding to the k^th principal component of the data matrix
RS: reconstructed signal

Statistical Process Control for threshold

Step1: The obtained reconstructed signal RS is decomposed using the discrete Wavelet packet decomposition. Then, the energy content of each node is calculated (similar to the multi-resolution analysis step) using equation 5.
Step 2: Calculate damage indicators SAD and SSD to be monitored instead of directly monitoring the change of the energy content (Sun 2002). SAD and SSD are defined (Sun and Chang 2004) as:
Sum of absolute difference (SAD) and computed as:

$$SAD(k) = \left| E(k) - E_{ref} \right| \tag{7}$$

Square Sum of Difference (SSD) and computed as:

$$SSD(k) = \left(E(k) - E_{ref} \right)^2 \tag{8}$$

With:
E_{ref} is the reference signal energy content over a healthy period before the monitoring period.
$E(k)$: the energy content of the RS at the monitoring time step k
Step 3: Apply SPC (statistical Process Control)
The X-bar control chart concept (Montgomery 1996) is used to established the threshold of damage indication. Thus Ang et al. suggest the following threshold calculation for a one-sided upper (1-α) upper confidence limit for the damage indicator SAD (a similar formula is calculated for SSD) (Ang and Tang 1975)

$$UL_{SAD}^{\alpha} = \mu_{SAD} + Z_{\alpha}\left(\frac{\sigma_{SAD}}{\sqrt{q}}\right) \tag{9}$$

Where:
UL_{SAD}^{α} : Upper Confidence Limit
μ_{SAD} : is the value toward which the mean value of the parameter SAD converges
Z_{α} : is the value of standard normal distribution with zero mean and unit variance, so that the cumulative probability is 100*(1-α)
σ_{SAD} : is the value toward which the standard deviation of the parameter SAD converges
q: interval of monitoring time
Then, X-bar control chart upper limit is used to monitor of the damage indicators over a given period of time.
The different statistical parameters are obtained after the system stabilized (see section 4. illustration)

Modified threshold calculation

In general, the control charts are effective in defect prevention (Montgomery 1996) when use in the context of manufacturing for example. However the authors have found that there is an overshoot in the value of the statistical parameters before converging for gas turbine application (see figure 8 for example) that is the use of the mean value of the SAD (μ_{SAD}) and the standard deviation of SAD (σ_{SAD}) directly may lead to an arbitrary higher number of false-positive alarms . Consequently, it is proposed to use the average of the 10 or so highest value of μ_{SAD} as the mean value. That consideration appears to reduce considerably the number of false alarms. Therefore the modified upper confidence limit for the damage indicator SAD is defined as:

$$UL_{SAD\_MX}^{\alpha} = \mu_{SAD\_MX} + Z_{\alpha}\left(\frac{\sigma_{SAD}}{\sqrt{q}}\right) \tag{10}$$

Bayesian Hypothesis for monitoring time

The Bayesian evaluation method is applied to the modified threshold value $\varepsilon = UL_{SAD\_MX}^{\alpha}$.
Thus, the Bayesian evaluation method for hypothesis testing is conducted with a binary outcome over a given period of monitoring time. The anomaly function is defined as H(t), which is the vector of the Bayesian hypothesis testing result with a null and an alternative hypothesis defined as follows:

- Null hypothesis H0:

$$SAD(t) \leq \varepsilon, H(t) = 1 \tag{11}$$

- Alternative hypothesis H1:

$$SAD(t) > \varepsilon, H(t) = 0 \tag{12}$$

The function H(t) has values of 1 or 0 and can be plotted over time for visualization. Thus H(t) value of 1 is a healthy state and a H(t) value of 0 is an abnormal one. Therefore, the appearance of the value of H(t) = 0 can be considered as a sign of failure precursor.

It is important for practical purposes to recalculate the threshold value (i.e. all the parameters used to calculate the threshold) after any exterior performance change as offline compressor water-wash, or installation of new parts or components

Type I and type II errors calculation

Recall that the probability of type I error or false-positive is defined as: α = P{reject H0|H0 is true};

That is the probability of detecting a failure precursor while there is no defect. Whereas, the type II error or false-Negative is defined as β = P{fail to reject H0|H0 is false}, that is the probability of missing a defect while one is present. In the proposed process the statistical confidence level or type I error is an input decided by the system operator; it has a probability of 100*(1-α)%.

To compute the type II error we assume H0 is false and H1 is true, and that the difference between mean values of the H0 distribution and the H1 distribution is δ. The type II error is the probability that the test statistic will fall between $-Z_{\alpha/2}$ and $Z_{\alpha/2}$ under H1 being true, as illustrated in figure 4. A more detail explanation of the concept of determination can be seen in (Montgomery 1985).

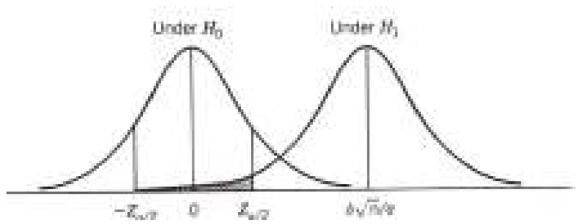

Figure 4: Graphical representation of type II Error

The type II error can be calculated using:

$$\beta = \Phi\left(Z_{\alpha/2} - \frac{\delta\sqrt{n}}{\sigma}\right) - \Phi\left(-Z_{\alpha/2} - \frac{\delta\sqrt{n}}{\sigma}\right) \tag{13}$$

Where:

Φ : is the cumulative standard normal distribution

δ : is the difference between the mean value used to calculate the threshold value and the mean value of the monitored interval of time of the damage indicator SAD and SSD.

σ : is the standard deviation

n: is the sample size

Another interesting statistical parameter is the process power defined as 1–β = P{reject H0|H0 is false}; it is the probability of correctly rejecting H0.

4 ILLUSTRATION

4.1 Test unit background

The proposed process is applied to a gas turbine compressor failure problem. 8 of the test unit sensors are considered and summarized in Table 1. The test unit failed on June 24, 2006 at 18:18. The gas turbine manufacturer found through a post compressor failure analysis that there was a failure precursor event (artificially big increased in sensor data) on June 20, 2006 at 23:30. Also, the manufacturer indicated that the operated hours of the unit were about one half the number hours required for inspection and that there were no major events prior to the compressor failure.

Table 1: Gas turbine health monitoring sensors

Sensors	Description
X1	Compressor health parameter 1
X2	Compressor health parameter 2
X3	Inlet guide vane (operating condition)
X4	Gas turbine output (system condition)
X5	Compressor seismic vibration 1
X6	Compressor seismic vibration 2
X7	Turbine seismic vibration 3
X8	Comp. inlet temp.(operation condition)

4.2 Methodology steps

***Step 1**:*

The sensor measurements for the 8 sensors of interest at 5-second intervals from June 19, 2006 at 00:00 to June 25, 2006 at 00:00 are obtained and presented in this study because there were no prior noticeable events.

***Step 2**:*

The raw data is normalized using the mean value of each variable (sensor). The normalized sensor readings are within the same order of magnitude with a mean value of 1 for each variable. Besides ensuring a concealment of the manufacturer proprietary data, another reason for normalizing the sensors measurement is to allow the analysis to not arbitrary be skewed toward variable with higher absolute values.

***Step 3**:*

All normalized raw sensor data is de-noised using DWPT.

***Step 4**:*

Each variable signal is decomposed into a 3-level tree as shown on Figure 4 using the DWPT and the "Daubechies 4" wavelet mother function (Chui 1992; Daubechies 1992). The energy content of each of the 8 nodes representing each wavelet component of the level 3 is calculated and serve as the signal feature characteristic. It observed that each of the 8 sensors has over 99.9% of its energy content at the approximation node, which is the node (3, 0) in Figure 4. Therefore, the approximation will be used as a representative of the actual signal in the subsequent steps.

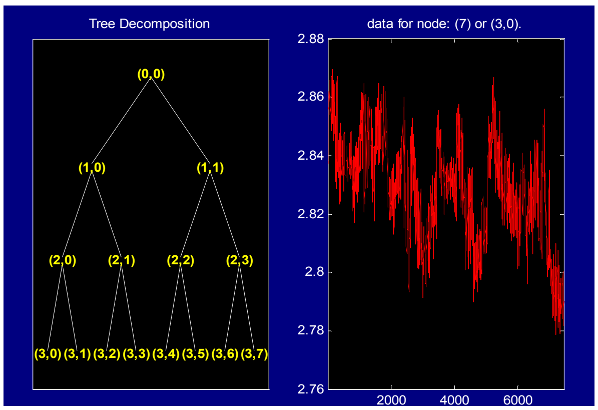

Figure 5: Tree decomposition of signal of variable X1

***Step 5**:*

The standard PCA steps are executed to determine the principal components (PC) which are the eigenvectors corresponding to the most significant eigenvalues of the covariance matrix formed with the sensor data. As shown on Figure 6, to maintain at least 95% of the original information in the model, the first 3 PCs representing 99.326% of the original information should be retained.

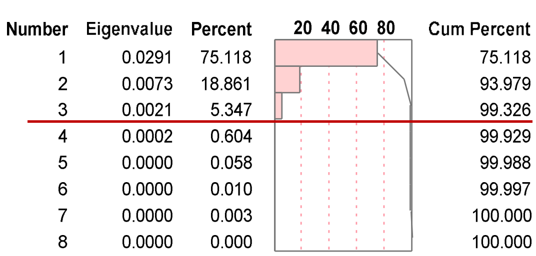

Figure 6: Pareto chart of eigenvalues contribution

Then the PPCA parameters are calculated with the maximum likelihood weight matrix first by setting to 0 any PC weight that is less than 0.1 as shown in table 2. Next the remaining PPCA parameters are computed (i.e. the isentropic noise covariance, the prediction error unique to response, the data matrix and the variance of reduced dimension).

Table 2: Maximum likelihood weight matrix

	3 Principal Components for 99.3%		
Variables	*PC1 (75.1%)*	*PC2 (18.9%)*	*PC3 (5.3%)*
X1	*0*	*0*	*0*
X2	*0*	*0*	*0*
X3	*0*	*0*	*0*
X4	*0*	*0*	*0*
X4	*0.59281*	*0.7203*	*-0.35998*
X6	*0.46975*	*0*	*0.88042*
X7	*0.65235*	*-0.69038*	*-0.30792*
X8	*0*	*0*	*0*

***Step 6**:*

This step deals with the anomaly detection:

- Computation of reconstructed signal

Since only the 3 most important principal components are kept, the reconstructed 1-dimensional signal is obtained as*:*

$$RS(t) = \lambda_1 \Phi_1^*(t) + \lambda_2 \Phi_2^*(t) + \lambda_3 \Phi_3^*(t) \qquad (14)$$

With λ_1=75.1%, λ_2=18.7% and λ_3=5.3%, which are the percentage of total information content in the 3 major eigenvalues.

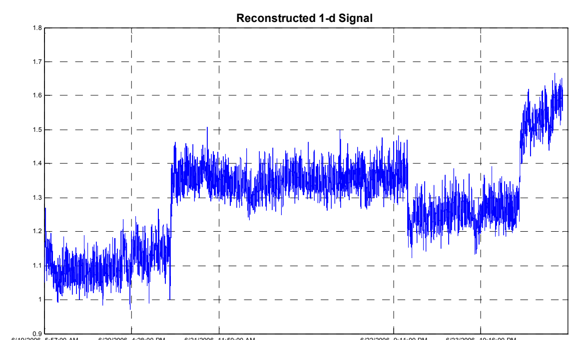

Figure 7: Reconstructed 1-d signal

The remaining analysis is based on the reconstructed 1-dimensional signal (RS), which is a representation of the original 8 sensors. The RS in turn is decomposed using the DWPT up to the level-3 decomposition, since higher level of decomposition did not yield any additional information

- *Threshold calculation*

To compute the damage indicators SAD and SSD, Eref needs to be established first. Eref is calculated as the mean value of the energy of the approximation node (3, 0) (representing more that 99.9% of the RS energy content) from the decomposed tree on figure 5 of the signal over one hour period using a 5-seconds time interval. Thus a value Eref=1.1328 is obtained.

Next, the mean and standard deviation values of SAD and SSD are needed to calculate the anomaly threshold. Therefore, SAD(k) is calculated at each time step and its value is added to a set in order to compute the mean and standard value of that set. Similar to the Eref calculation, E(k) represents the energy content of the node (3,0) (3 –level of decomposition) at each time step k. The calculation is repeated over time until the mean value and standard deviation of the set SAD values converge towards μ_{SAD} and σ_{SAD} respectively as shown on figure 8.

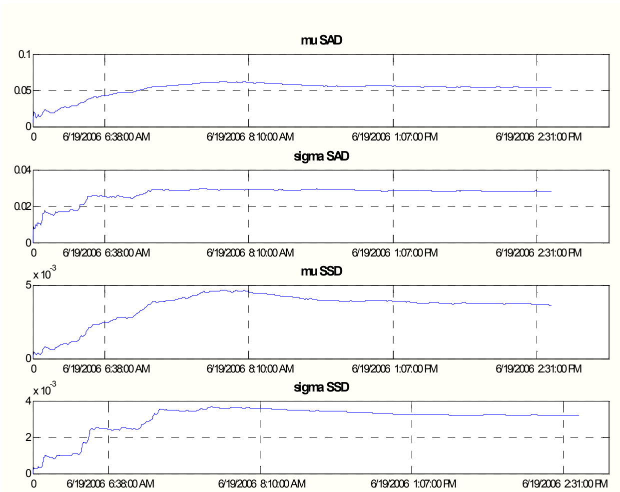

Figure 8: Convergence of mean and standards deviations of SAD & SSD

After the statistical parameters convergence, the modified mean value of SAD=0.1332 is obtained. And the threshold of SAD is calculated as ε =0.1337. In a similar way the parameters for SSD are obtained.
The remaining parameters to calculate the threshold are α and q. In the case of this illustration, values of α=0.02 and q=12000 which corresponds to a monitoring time of over 16.6 hours (green curve on figure 9) are used.

The idea is that, once the threshold (red dash line) is set, a system operator monitors the SAD (or the SSD) signal (green curve) instead of the original 8 sensors, and any time the value of SAD goes above the calculated threshold, it is considered an anomaly.
The figure 9 below shows the threshold, the magnitude and length of anomalies and the point of the catastrophic failure.

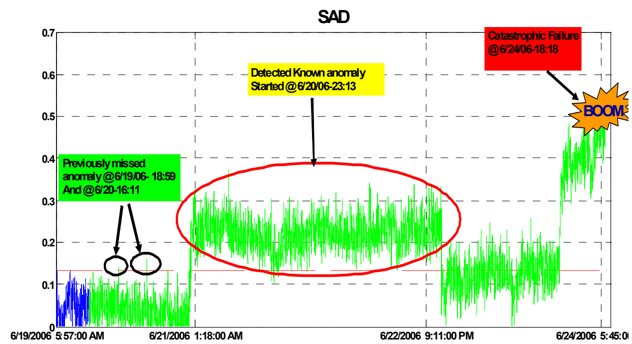

Figure 9: SAD parameters with detected anomalies

- Bayesian Hypothesis Testing

The final step is the Bayesian hypothesis testing. The result is the binary function H(t) with entry values of "1" and "0". As shown on the figure 10, there are four abnormal events during the almost 17 hours of monitoring. In a post-processing analysis, the gas turbine manufacturer established that the initial indication of a precursory event that led to the compressor failure was on 06/20/2006 at 23:30.
Indeed, the proposed not only successfully detected that event but found it started precisely at 23:13 (that 17 minutes before the OEM time). More importantly, the proposed approach is capable of capturing that severity and length of anomalies. Furthermore, the proposed process has detected three other less severe and short lasting defects as marked on figure 10 missed by the gas turbine manufacturer's procedure, the first of which was more than 24 hours before the manufacturer's first detect anomaly.

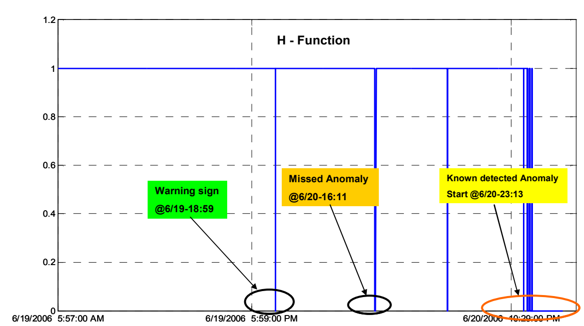

Figure 10: Result Bayesian hypothesis testing

Finally, the errors associated with the precursor detection are calculated. Since the probability of false-positive is an input that is decided but the analysis and it represent 2% in this example, the probability of type II error or false-negative is calculated to be less than 10e-4 that is much smaller; which meets the goal of a practical process that to be implemented has to have a much smaller type II error for given type I error.

5 CONCLUSION

The LTSA market can be a very lucrative one if the level of liquidated damage is managed to a minimum cost. In this paper, a systematic approach is offered to detect precursory anomalies that could lead to catastrophic gas turbine compressor failure in an effort to reduce or even eliminate unplanned power plant outages. The proposed approach is very promising as it has successfully detected previously known failure precursory anomalies as well as the ones missed by the manufacture analysis.

The proposed approach can be easily implemented unlike other techniques that rely on the use of neural network, where a high fidelity mathematical model is required. Furthermore, the process appears to be robust with few false alarms and a much lower false-negative probability for given rate of false-positive. Additionally, the use of the statistical approach allowed the handling practical issues of heavy duty gas turbines such as machine-to-machine variation and the wide variation in operation condition. Importantly, the proposed methodology has the ability to not only detect an anomaly, but also its severity and its length which can help trained technicians make the right decisions.

Overall the proposed approached is a novel one as it is based on the fusion of information from both health parameter sensors as well vibration sensors, whereas current industry standard relies solely on vibration sensors. Consequently any defect that has no vibration signature would be missed by the current OEM's analysis. Thus in the illustrative example, the first sign of a malfunction is detected about five full days before the actual machine catastrophic failure, which is more than enough time needed to avoid the failure.

ACKNOWLEDGMENT

The authors would like to thank GE Energy for providing gas turbine data.

REFERENCES

Ang, A. and W. Tang (1975). "Probability concepts in engineering planning and design."

Chui, C. (1992). An introduction to wavelets, Academic Pr.

Daubechies, I. (1992). Ten lectures on wavelets, Society for Industrial Mathematics.

Diallo, O. and D. Mavris (2010). A Concept for Intelligent Fault Detection Using a Multi-resolution Analysis. Aerospace Systems Conference, Los Angeles, CA.

EPRI (2007). Gas turbine compressor dependability: investigation of the MS7001F /9001F R0 compressor stage blade designs and failures, Electric Power Research Institute (EPRI).

EPRI (2008). GE FA Compressor Dependability (phase 2), Electric Power Research Institute (EPRI).

Graps, A. (1995). "An introduction to wavelets." IEEE Computational Science & Engineering **2**(2): 50-61.

Jiang, X. and H. Adeli (2004). "Wavelet packet-autocorrelation function method for traffic flow pattern analysis." Computer-aided civil and infrastructure engineering **19**(5): 324-337.

Jiang, X., S. Mahadevan, et al. (2006). "Bayesian wavelet packet denoising for structural system identification." Progress in Structural Engineering and Materials **14**(2): 333-356.

Matlab (1999-2009). Wavelet Toolbox 4 -User's Guide. Matlab 7.8.0 (R2009a).

Misrikhanov, A. (2006). "Wavelet transform methods: Application in electroenergetics." Automation and Remote Control **67**(5): 682-697.

Montgomery, D. (1985). "Introduction to statistical quality control."

Montgomery, D. (1996). Introduction to statistical quality control, Wiley- New York.

Stoll, H. (2001). "Creating owner's competitive advantage through contractual services." GER-4208, GE Power Systems.

Sun, Z. (2002). "Structural damage assessment based on wavelet packet transform." Journal of structural engineering **128**: 1354.

Sun, Z. and C. Chang (2004). "Statistical wavelet-based method for structural health monitoring." Journal of structural engineering **130**: 1055.

Thaler, H. (2006). Global Gas Turbine Markets and Trends - What does the future hold? The Future of Gas Turbine Technology - 3rd International Conference, Brussels.

Tipping, M. and C. Bishop (1999). "Probabilistic principal component analysis." Journal of the Royal Statistical Society. Series B, Statistical Methodology: 611-622.

Wu, Y. and R. Du (1996). "Feature extraction and assessment using wavelet packets for monitoring of machining processes." Mechanical systems and signal processing **10**(1): 29-53.

Ousmane Diallo: and was born in Abidjan, Cote d'Ivoire. He is currently a PhD candidate in the Aerospace Systems Design Laboratory under Prof. Dimitri Mavris at the School of Aerospace Engineering in the Georgia Institute of Technology.